Available online at www.sciencedirect.com
ScienceDirect
Journal of Applied Geophysics 62 (2007) 33–46
JOURNAL OF APPLIED GEOPHYSICS
www.elsevier.com/locate/jappgeo

Hydraulic conductivity estimation from induced polarisation data at the field scale — the Krauthausen case history

Andreas Hördt [a,*], Roland Blaschek [a], Andreas Kemna [b], Norbert Zisser [c]

[a] *Institute of Geophysics and Extraterrestrial Physics, TU Braunschweig, Mendelssohnstr.3, 38106 Braunschweig, Germany*
[b] *Agrosphere, ICG-IV, Forschungszentrum Jülich GmbH, 52425 Jülich, Germany*
[c] *University of Bonn, Mineralogisch-Petrologisches Institut, Poppelsdorfer Schloss, 53115 Bonn, Germany*

Received 23 March 2006; accepted 7 August 2006

Abstract

Recently, encouraging results have been obtained to estimate hydraulic conductivity in unconsolidated sediments from induced polarisation (IP) measurements. The work focussed on laboratory experiments in order to establish semi-empirical relationships between complex electrical conductivity and hydraulic parameters. Although field studies are certainly important to evaluate the feasibility of the method in practice, only a limited number of case histories have been reported. We carried out an IP survey at the Krauthausen hydrogeological test site in Germany. Multifrequency data were recorded along two profiles with a dipole–dipole configuration and 2 m electrode spacing. The data were inverted with a 2-D inversion code to obtain images of conductivity magnitude and phase for each frequency. We used a novel focussing regularisation scheme that does not suppress sharp boundaries and yields realistic images of the subsurface. The gross structural features compare well with the known lithology, which consists of an approx. 9 m thick sand/gravel aquifer over fine sands and a thin clay layer which constitutes the base at approx. 11 m depth. From the complex electrical conductivity distribution we calculate hydraulic conductivity estimates using the empirical equations suggested by Börner et al. [Börner, F. D., Schopper J. R., Weller, A., 1996. Evaluation of transport and storage properties in the soil and groundwater zone from induced polarisation measurements. Geophys. Prosp. 44, 583–601] and by Slater and Lesmes [Slater, L. D., Lesmes, D. P., 2002a. Electric hydraulic relationships observed for unconsolidated sediments. Water Res. Research, 38 (10), doi:10.1029/2001WR001075] and compare the results with values obtained from grain size data at two boreholes. The Börner model yields hydraulic conductivities in the same order of magnitude as the grain size data, whereas the Slater and Lesmes model substantially underestimates hydraulic conductivities. We also compare the specific inner surface estimated from our IP data with values obtained from BET measurements at the two borehole locations. In this case, we observe a reasonable agreement with both the Börner and the Slater and Lesmes equations. Our results constitute an encouraging example where reasonable estimates of hydraulic parameters are obtained at the field scale.
© 2006 Elsevier B.V. All rights reserved.

Keywords: Induced polarisation; Complex conductivity; Hydraulic conductivity; Spectral IP; Groundwater

1. Introduction

Hydraulic conductivity is an essential parameter in hydrogeology, used for groundwater management, groundwater protection and prediction of contaminant

* Corresponding author.
E-mail addresses: a.hoerdt@tu-braunschweig.de (A. Hördt), a.kemna@fzjuelich.de (A. Kemna).

0926-9851/$ - see front matter © 2006 Elsevier B.V. All rights reserved.
doi:10.1016/j.jappgeo.2006.08.001

transport. Standard techniques to determine hydraulic conductivity, such as well tests, permeameter measurements and grain size analyses, are invasive, some are relatively expensive, and either integrate over a large volume or provide information only in the vicinity of the boreholes. Therefore, good estimates of hydraulic parameters from surface geophysical measurements could provide important complementary information and might help to reduce the costs of hydrogeological investigations. The use of DC resistivity methods alone may be feasible in particular situations where a lot of a priori information is available, but in general, a unique relationship between DC resistivity and hydraulic conductivity does not exist (e.g. Mazac et al., 1985; Purvance and Andricevic, 2000). The reason is that hydraulic parameters depend on both porosity and geometry of the pore space, which cannot be uniquely determined with DC resistivity alone without further assumptions. The application of the induced polarisation (IP) method is an attempt to gain more information about the pore space by measuring chargeability (in the time domain), or, equivalently, the phase shift between current and voltage (in the frequency domain) in addition to the DC resistivity.

Several authors have suggested semi-empirical relationships between IP parameters and hydraulic conductivity. Börner et al. (1996) estimate hydraulic conductivity from the formation factor and the inner surface area, using a Kozeny–Carman type (Schön, 1996) equation. Their model, hereinafter called "Börner model" for convenience, requires the complex electrical conductivity distribution only at a single frequency around 1 Hz, and the groundwater electrical conductivity. Slater and Lesmes (2002a) found that grain size exerts the primary control on complex conductivity and suggested an alternative model based on a correlation between imaginary conductivity and grain size, without using the formation factor. Both models require the assumption or calibration of several model parameters, as will be discussed below.

Only a limited number of systematic studies exist to determine hydraulic conductivity from IP measurements at the field scale. Börner et al. (1996) applied their empirical equations to data obtained in small boreholes and from IP soundings, and compared the results with grain size determined hydraulic conductivities. Kemna et al. (2004) applied the Börner model and the Slater and Lesmes model to data from crosshole IP imaging and compared the results with lithological information. They also suggested an extension of the Börner model to include saturation. Slater and Glaser (2003) carried out laboratory measurements and a crosshole IP survey over a sandy aquifer. They used the Börner model to estimate hydraulic conductivities and obtained a good agreement with lithologic information. These studies indicated that IP measurements may provide order of magnitude estimates of hydraulic conductivity. However, they were naturally limited to certain lithologies, and more experience at the field scale with different lithologies and a systematic evaluation at the field scale is certainly desired. Moreover, it is always difficult, if not impossible, to maintain soil samples in the same condition as they are in the field, and thus field studies constitute an essential step towards practical application.

Here, we present a case history where we use multichannel surface IP measurements over a sand/gravel aquifer at the hydrogeological test site Krauthausen, Germany. Although we carried out measurements over a broad frequency range, in which case the measurements are called spectral IP (SIP), we restrict the hydraulic conductivity analysis to single frequency data, following the Börner model and the Slater and Lesmes model. Laboratory measurements typically use frequencies between 0.01 Hz and 1 kHz (e.g. Börner et al., 1996; Slater and Lesmes, 2002a; Slater and Glaser, 2003; Kemna et al., 2005). Recently, theoretical models have been developed to relate grain size or pore radii distributions to parameters derived from the spectral information (Lesmes and Morgan, 2001; Titov et al., 2002; Klitzsch, 2004). However, in the field, the frequency range is limited by induction effects at high frequencies and acquisition time at low frequencies. In the useful range, our data show only small phase variations. Our main scope at this stage is to use the robust piece of information and evaluate equations that have been set up in the laboratory by comparing the estimated hydraulic conductivities with values obtained from grain size analyses.

2. The method and the survey

The spectral induced polarisation (SIP) technique is based on the same principles as DC resistivity methods. The difference is that an alternating current is injected instead of a DC current, and the phase shift between voltage and current signals is measured in addition to the resistance (amplitude ratio). The data consist of apparent resistivity magnitude and phase for each frequency, which may be inverted to obtain resistivity (or conductivity) magnitude and phase images of the subsurface for each frequency. Here, we will present raw data in terms of resistivity, but for pseudosections and interpretation we will consistently use complex conductivity,

because this form is convenient for hydrogeological applications:

$$\sigma = |\sigma| e^{i\varphi} = \sigma' + i\sigma'', \quad (1)$$

where σ' and σ'' denote real and imaginary part, and $|\sigma|$ and φ denote magnitude and phase, of the complex conductivity σ.

Induction effects are assumed to be negligible. If this assumption holds, the frequency dependence of the measured voltage is solely governed by the frequency dependence of the subsurface conductivity, and can be calculated by solving a separate DC problem with complex conductivities for each frequency (e.g. Weller et al., 1996). Recent reviews of the method including a brief discussion of the underlying conduction mechanisms can be found in Slater and Lesmes (2002b), Kemna et al. (2004), and references therein.

The test site Krauthausen is situated about 10 km northwest of Düren, Germany. The extension of the site is 200 m × 70 m, and the topography is flat. The site is operated by the Agrosphere, ICG-IV, Forschungszentrum Jülich, Germany. It has been investigated in detail by drillings, grain size analyses, tracer tests and geophysical methods, and the hydrogeological situation is well known (Vereecken et al., 2000; Englert et al., 2000). Fig. 1 shows the average lithology. The gross structure consists of an approx. 9 m thick aquifer, with the base at approx. 11 m, and a surface soil layer above. The groundwater table was at 2.1 m depth when the present survey was conducted. The aquifer is characterised by different layers of sand and gravel corresponding to Rur sediments, partly exhibiting a strongly non-uniform grain size distribution (i.e. with both very small and large grains) (see Vereecken et al., 2000, for more details). A clay layer at approx. 11 m depth forms the base of the aquifer, followed by fine sands corresponding to Upper Rhine sediments.

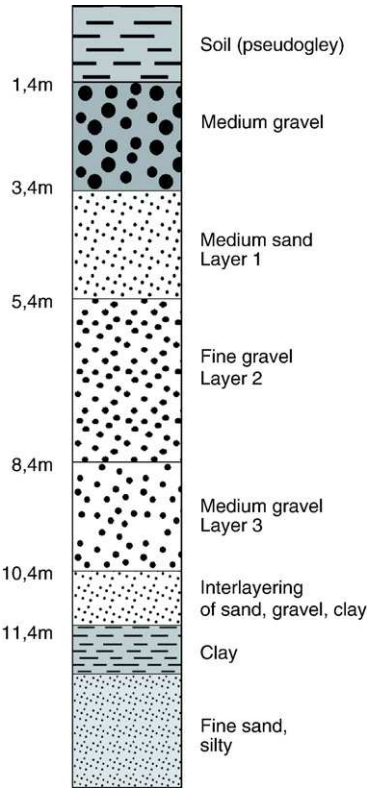


Fig. 1. Lithology of the Krauthausen test site, modified after Vereecken (2000), Döring (1997) and Englert (pers. comm.). Layer 1, 2 and 3 correspond to the nomenclature in Vereecken et al. (2000).

Spectral induced polarisation measurements were carried out along several profiles (Fig. 2). Two of the profiles are crossing the locations of two particular boreholes (b32 and b22) where detailed grain size data are available. These data were recorded with a broad frequency range from 76.22 mHz to 500 Hz. In addition, 10 profiles were recorded with a single frequency (1 Hz) at a dense spacing of 2 m in order to obtain a high coverage, possibly allowing for a later 3-D inversion. These data will not be discussed here, but results based on 2-D inversions were shown by Hördt et al. (2005).

We used the multichannel equipment SIP256C by Radic Research (Radic et al., 1998; Radic, 2004). A typical field set up is shown in Fig. 3. Each steel electrode is connected to a remote unit and can both inject current and measure the potential. The remote units carry out the voltage or current measurements, digitise the data and transfer them to the controlling PC through a fiber optics cable to avoid interference of the current supply cables with the voltage measurement. The optimum measurement strategy is constrained by two factors. First, induction effects may be minimised by using a dipole–dipole configuration rather than the common Schlumberger or Wenner geometries. Second, when using steel electrodes, an electrode that has been used for current injection cannot be immediately used for voltage measurements because of transient polarisation effects (e.g., Dahlin et al., 2002). This leads to a dipole–dipole configuration with a particular sequence of transmitting dipoles moving along the profile, where the data recorded by electrodes that have previously transmitted are usually ignored. Our own experiments (not shown) confirmed that non-polarising electrodes perform no better than steel electrodes if we follow the guidelines outlined above. We used 32 electrodes at 2 m separation, and a basic dipole length of 2 m.

Fig. 4 shows a sample data set displayed as magnitude and phase of complex apparent resistivity vs. frequency.

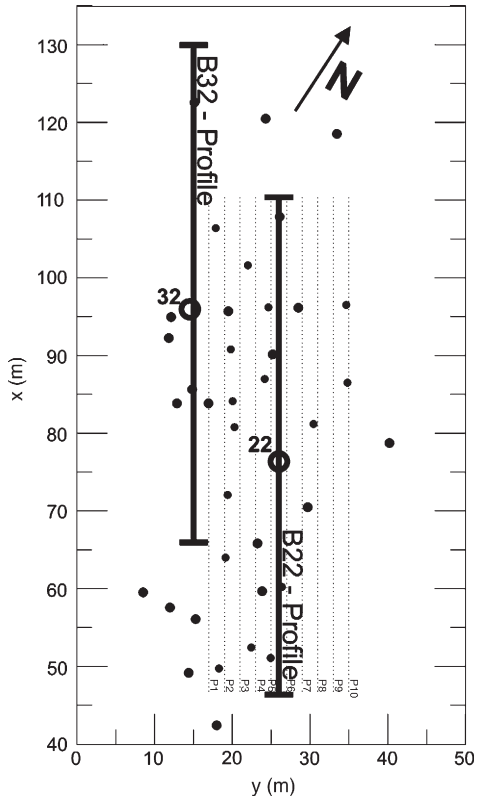


Fig. 2. Survey configuration at the Krauthausen test site. The dots denote borehole locations. Detailed grain size information is available at boreholes b22 and b32. Results from the two profiles crossing b32 and b22 are discussed here. The open square indicates the borehole where a pump test was carried out (after Englert et al., 2000).

The magnitude decrease with frequency is expected, because polarisation is an additional conductivity mechanism that becomes more efficient at higher frequencies. Note that a narrow resistivity range is displayed to enhance the small variation of less than 3%. The resistivity phase, shown in milliradian, is almost constant over a wide frequency range (up to 10 Hz) and shows a strong decrease (increasing absolute values) at higher frequencies. This is not due to the intrinsic variation of conductivity with frequency, but rather due to inductive or capacitive coupling. Induction may be ignored if either the frequencies or the transmitter–receiver spacings are sufficiently small, depending on the conductivity of the ground. Attempts have been made to remove inductive effects from the data (Pelton et al., 1978; Kemna et al., 1999; Xiang et al., 2002), but here we use the data only in the range below 10 Hz where the data are not significantly affected. Capacitive coupling effects are particularly important when the contact resistance of the electrodes is high. Radic (2004) discusses different kinds of coupling and suggests measures to avoid or reduce them. Both inductive and capacitive coupling can cause the observed increase of absolute phases (e.g. Hallof, 1974; Radic, 2004) and thus it cannot be decided without further investigation which one is dominating.

Acquisition of low-frequency data is limited by the data acquisition time. At our lowest frequency of 0.076 Hz, recording 5 periods was sufficient to obtain a satisfactory data quality (i.e. a phase error not larger than approx. 0.3 mrad for the largest transmitter–receiver distance (30 m) used in the inversion). This amounts to more than one minute recording time at this frequency, and several seconds have to be added for data transfer and storage. Acquisition time for one profile is several hours and can easily become excessive if lower frequencies are required, even though the system efficiently measures voltages at all receiver channels simultaneously.

3. 2-D inversion

A 2-D inversion of the data was carried out for a selected frequency. The subsurface is subdivided into cells with constant model parameters, consisting of intrinsic magnitude and phase of the complex conductivity. The inversion is based on the approach by Kemna and Binley (1996) and Kemna (2000). The main features of the original code (Kemna, 2000) are a forward solution based on finite elements and a standard Gauss–Newton inverse scheme with smoothness-constrained regularisation, both using complex calculus. However, since the smoothness constraint produces images with smooth parameter transitions even if there is a sharp lithological boundary, we implemented a modified version of the minimum gradient support (MGS) regularisation suggested by Portniaguine and Zhdanov (1999). This regularisation does not suppress sharp boundaries and yields focussed images that typically consist of well separated zones with smooth parameter variations within. In our modification, we allowed for a variation of a control parameter to obtain a continuous transition between focussed and smoothness-constrained results. The freedom to choose between models with a different degree of smoothness in principle makes the approach subjective. In this particular case we used a standard value for the control parameter that was previously determined as optimum from inversion experiments with synthetic data. We further extended the regularisation to include sensitivities following an idea by Yi et al. (2003), to preserve the focussing properties even where sensitivities are low. Details of the complete regularisation scheme are given in Blaschek et al. (2005), and an in-depth discussion of



Fig. 3. The multichannel SIP equipment by Radic Research (Radic, 2004) in operation at a field site in North Germany. The white boxes are remote units that control the electrodes and digitise the data before sending them to a PC through a fibre optics cable.

the properties can be found in Blaschek (2006) and will be subject of a separate paper.

Both regularisation schemes (smoothness-constrained and modified MGS) produce similar data fits, which is why we show only the data fit of the modified MGS inversion in Fig. 5. We chose the 312 mHz data for presentation and further discussion, because they have the best signal-to-noise ratio in the frequency range around 1 Hz, which is used as a reference value by Börner et al. (1996) and Slater and Lesmes (2002a). The data are presented as pseudosections of apparent conductivity magnitude and phase. The inversion algorithm fits the logarithm of the complex apparent conductivity data; for the shown pseudosection these log data were fitted to an assumed error floor of 1% for the magnitude and 0.3 mrad for the phase values. Trying to fit the data below this error level results in deteriorated convergence and unrealistic models. Because measured and calculated (i.e. predicted by the inverted model) pseudosections agree very well and cannot be distinguished visually, we show the difference instead of the calculated data in the bottom panel.

The apparent magnitude section (Fig. 5, top left panel) exhibits a predominantly layered structure, with lateral variations within the layers. There are also linear diagonal features apparently caused by near surface conductivity anomalies. The difference section (Fig. 5, bottom left panel) ideally would show a random distribution. Instead, it is characterised by relatively large deviations for the short spacings (near surface) and by diagonal features. Although the differences are small and the data fit is excellent, the figure shows that systematic errors are more important than random noise. The phase pseudosection (Fig. 5, top right panel) is dominated by the diagonal features and does not exhibit a clear layering. The inversion is able to simulate those effects, and the remaining systematic structures in the difference section (Fig. 5, bottom right panel) are below 1 mrad.

The model obtained with the smoothness-constrained inversion is shown in Fig. 6 in the form of conductivity magnitude and phase, and the imaginary part σ''. Displaying all three parameters is redundant, because only two of them are independent, i.e. the σ'' image is approximately equal to the multiplication of the two others. Previous work has shown that phase and imaginary conductivity images may reflect different subsurface characteristics and thus looking at both of them can be instructive (e.g. Kemna et al., 2004). Below the resistive soil, the conductivity magnitude monotonically increases with depth. The conductivity phase behaves differently, showing a layer with small values roughly between 6 and 11 m depth, embedded between zones of higher phase shifts above and below. The qualitatively different behaviour with depth means that the phase data contain complementary information. The imaginary conductivity combines both sections, but is dominated by the conductivity magnitude which leads to a continuous increase with depth. Since, as will be discussed below, σ'' increases with the pore space-related internal

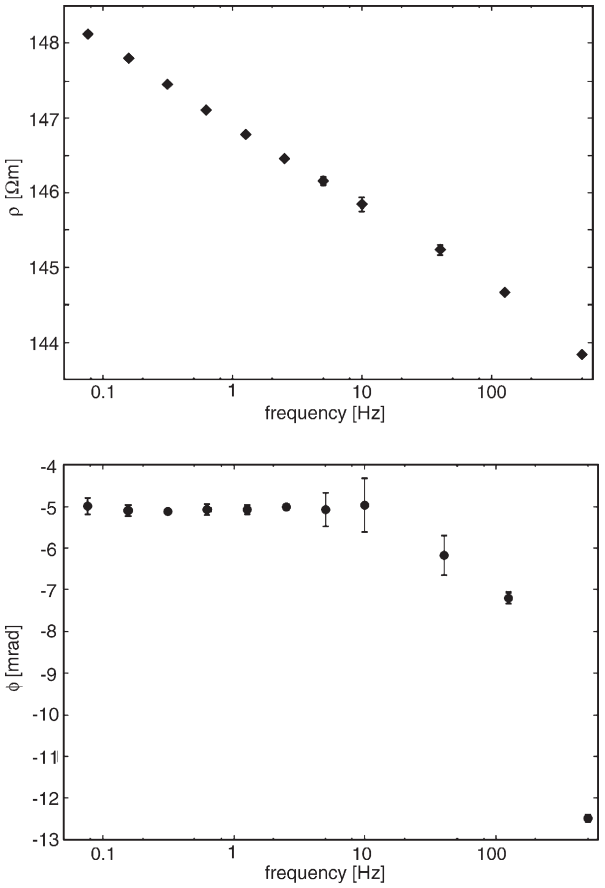


Fig. 4. A sample complex apparent resistivity data set from the Krauthausen test site. The transmitter and receiver dipoles are 2 m in length, the spacing is 24 m. Top panel: resistivity magnitude vs. frequency. Bottom panel: resistivity phase shift vs. frequency. The error bars are determined from the statistics of the stacking procedure during data acquisition.

surface, S_{por} of the sediments and the hydraulic conductivity varies inversely with S_{por}, the increase of σ'' with depth corresponds to a decrease of hydraulic conductivity. This is in qualitative agreement with the lithological information (Fig. 1). However, due to the smoothness constraint, the different layers are not well defined and cannot easily be related to the known lithology. In particular, we expect a well defined, sharp boundary in approx. 11 m depth, representing the base of the aquifer. Thus, although the model explains the data, the smoothness-constrained inversion result does not look like a realistic image of the subsurface.

Fig. 7 shows the model obtained with the modified MGS regularisation. Qualitatively, the result looks similar to the smooth inversion model, but now the images reflect the anticipated geology much better: well defined zones, predominantly horizontal, and smooth lateral variations within the zones. The images look more realistic than the smooth inversion results, and coincide well with the known average lithology given in Fig. 1. The sediments between 1 and 3 m depth appear as a distinct layer with low conductivity magnitude and high phase shifts. The base of the aquifer appears in the phase image as a sharp boundary, whereas it is less prominent in the conductivity magnitudes. In the σ'' image, which will be the basis for hydraulic conductivity estimation, the multiplication of the magnitude with the phase enhances the aquifer base. There is little discrimination in the range between 4 and 11 m, indicating that electrical (and likewise hydraulic) property variations within the aquifer are below the resolution limit of the method.

Fig. 8 shows the inversion result for the parallel profile crossing borehole b22, obtained with the modified MGS regularisation. The images are qualitatively similar to the b32 images (Fig. 7), with the aquifer characterised by low phase values and intermediate conductivities, overlain by a more inhomogeneous layer with higher phase values and low conductivities. The data fit (not shown here) is comparable to the fit of the b32 profile, using the same error levels of 1% and 0.3 mrad, respectively.

4. Hydraulic conductivity estimation

We used two different approaches to estimate hydraulic conductivities from the IP results. The first was suggested by Börner et al. (1996) based on laboratory measurements on unconsolidated sediments. They found that the phase shift for most of their samples was practically constant over a broad frequency range and called their model the "constant-phase-angle" (CPA) model. In that case, real and imaginary parts of complex electrical conductivity for one frequency (preferably around 1 Hz) are sufficient to estimate hydraulic conductivity. First, the formation factor, F, is calculated:

$$F = \frac{\sigma_w}{Re(\sigma) - \mathrm{Im}(\sigma)/l} \tag{2}$$

where σ_w is the pore fluid conductivity. The factor l is the ratio between imaginary and real part of the surface conductivity. It is used as an adjustable parameter to correct for the contribution of surface conductivity to the bulk real conductivity. Börner et al. (1996) suggest to use $l=0.1$ in unconsolidated sediments. The second important parameter is the pore space-related internal surface area, S_{por}, given by:

$$S_{por} = 8.6 \cdot 10^4 \sigma'' \tag{3}$$

where σ'' is given in S/m and S_{por} in μm^{-1}. Eq. (3) was empirically derived from laboratory measurements. It

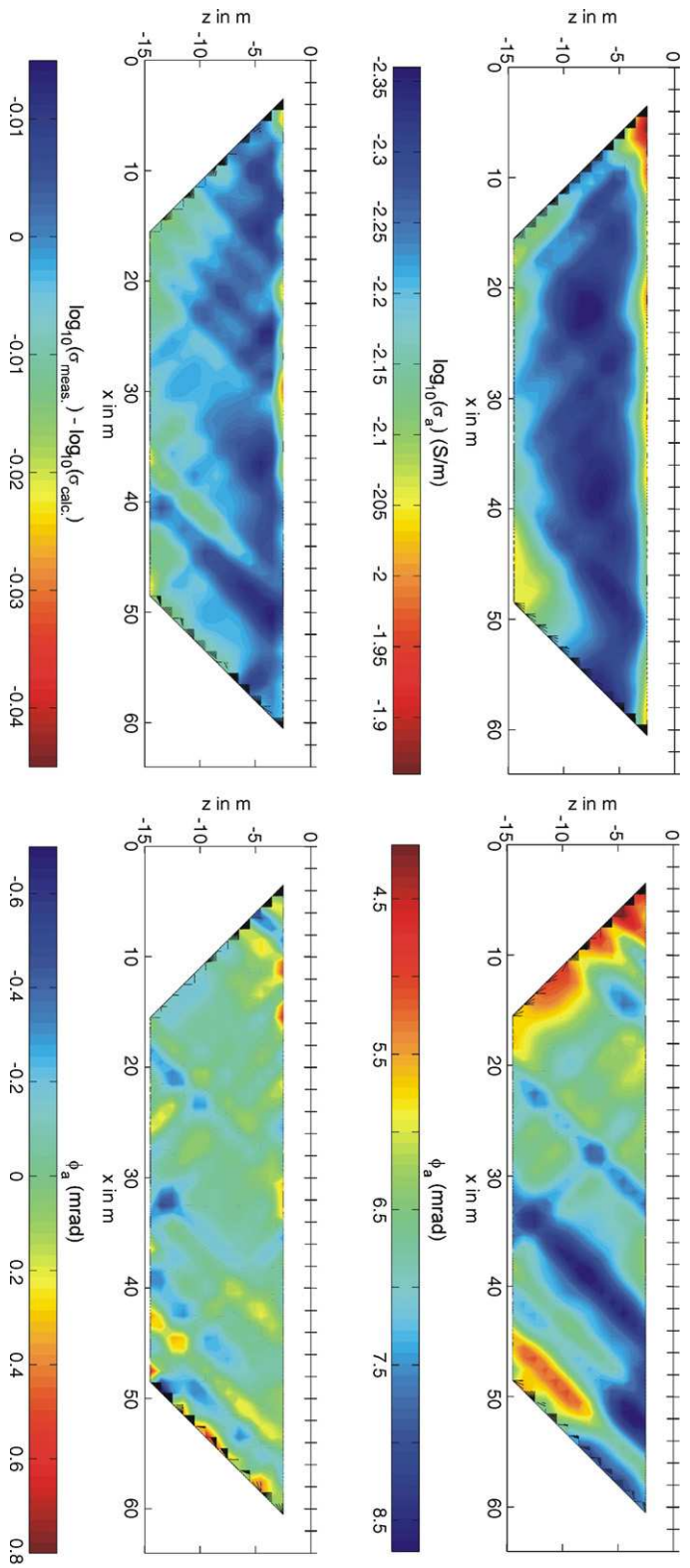


Fig. 5. Left: measured (top) and difference between measured and calculated (bottom) apparent conductivity magnitude pseudosection at 312 mHz along profile b32. Right: measured (top) and difference between measured and calculated (bottom) conductivity phase pseudosection at 312 mHz.

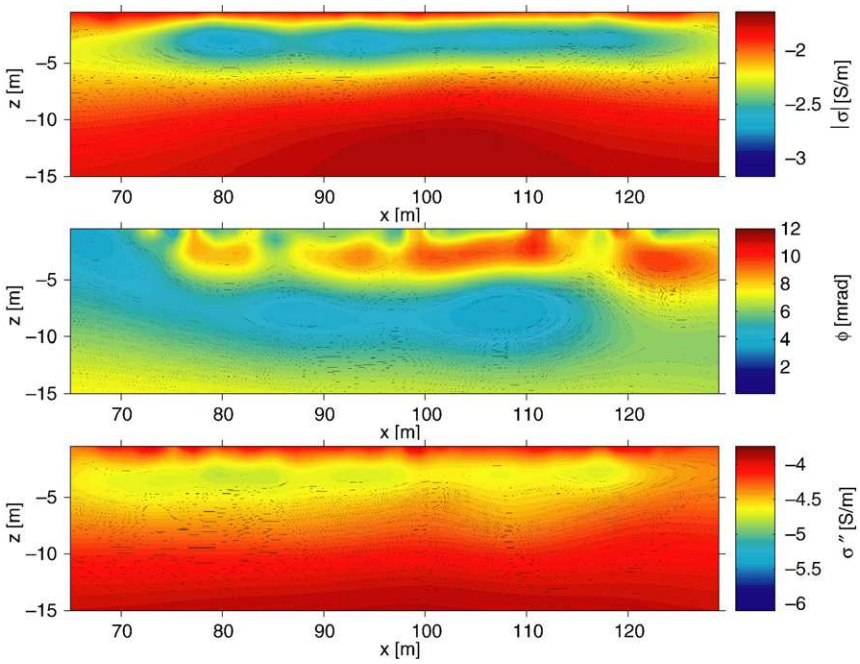


Fig. 6. Smooth 2-D complex conductivity inversion model at 312 mHz along profile b32 (at 96 m). The profile coordinates correspond with the map in Fig. 2. The corresponding data fits are shown in Fig. 5. Top: log10 of conductivity magnitude. Middle: conductivity phase shift. Bottom: log10 of imaginary part of conductivity.

has not been investigated in detail how well this linear relationship between surface area and imaginary conductivity performs if applied to other sediments than those used in that particular study. Examples have been reported where a power law gives a better fit to the data (e.g. Slater and Lesmes, 2002a). Here, we wish to assess

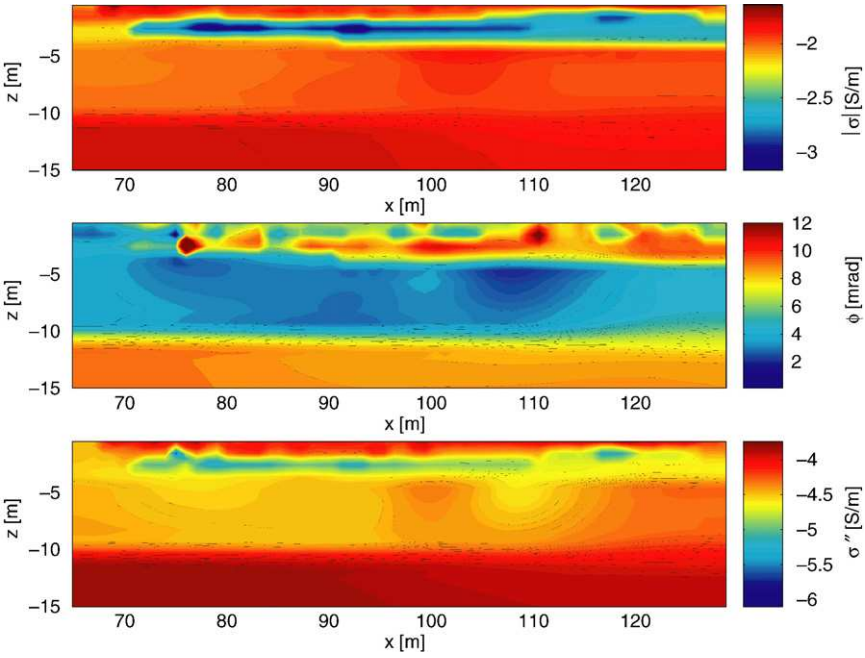


Fig. 7. Focussed (using modified MGS regularisation) 2-D inversion model at 312 mHz along profile b32 (at 96 m). Top: log10 of conductivity magnitude. Middle: conductivity phase shift. Bottom: log10 of imaginary part of conductivity.

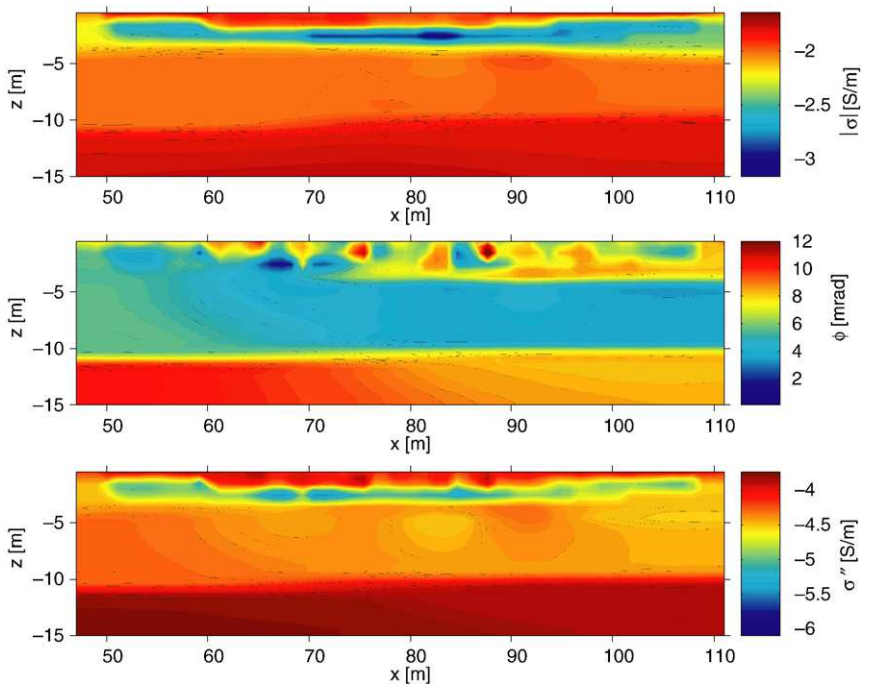


Fig. 8. Focussed 2-D inversion model at 312 mHz along profile b22 (at 76 m). Top: log10 of conductivity magnitude. Middle: conductivity phase shift. Bottom: log10 of imaginary part of conductivity.

the equations in their original form, and thus proceed with Eq. (3). The formation factor and specific inner surface area then enter into a Kozeny–Carman type of equation to calculate hydraulic conductivity, k:

$$k = \frac{1}{F(S_{\mathrm{por}})^c}, \tag{4}$$

where k is in m/s and S_{por} in $\mu\mathrm{m}^{-1}$. The exponent c is another adjustable parameter experimentally found to be in the range between $2.8 < c < 4.6$ (Börner et al., 1996), depending on the method of permeability measurement. Since this is a relatively broad range for an exponent which strongly influences the result, we investigated its influence and adjusted it using granulometric data obtained from two different boreholes.

The second approach was suggested by Slater and Lesmes (2002a). They used laboratory studies with both natural sediments and artificial mixtures of sand and clay. They argue that the hydraulic conductivity primarily depends on the specific inner surface, and set up an empirical relationship directly between k and the imaginary part of conductivity at 1 Hz, without using the real part and/or the formation factor:

$$k = \frac{m}{(\sigma'')^n} \tag{5}$$

Here, σ'' is given in $\mu S/m$, m and n are adjustable parameters with $m = (2.0 \pm 0.3)\ 10^{-4}$; $n = 1.1 \pm 0.2$, and k is in m/s. Note that Eqs. (4) and (5) have the same form with respect to the σ''-dependence, but the exponent is significantly smaller in the Slater and Lesmes model. Also note that Slater and Lesmes (2002a) obtain a much smaller range for the exponent from their data than Börner et al. (1996).

Fig. 9 shows the hydraulic conductivities estimated from the 2-D inversion result shown in Fig. 7 at the location of borehole 32, using both the Börner and the Slater and Lesmes models. First, note that the results are valid only below the groundwater table as indicated in the figure, because all the equations given above assume saturated conditions. Kemna et al. (2004) extended the Börner equations to include saturation. We did not attempt to consider saturation here, because we focus on the depth range between 3 and 11 m of the aquifer, below the groundwater table (approx. 2 m depth) and below the medium gravel layer which has large uniformity coefficients.

There are several empirical equations to determine hydraulic conductivity from grain size data, some of which are valid for a certain range of uniformity coefficients of the grain size distribution only. For the lithology here, the equation by Seiler (1979), using the

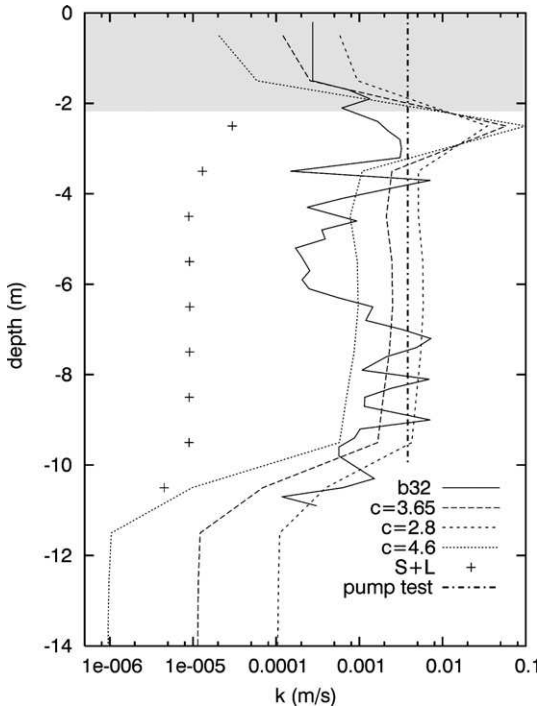


Fig. 9. Hydraulic conductivity at the location of borehole 32. Solid line: from grain size data using the Seiler-10 equation. Dashed lines: from the Börner model using different values of exponent c. Symbols: from the Slater and Lesmes model. Dash-dotted line: result from a pump test (Englert et al., 2000). The shaded area denotes the unsaturated zone where the equations are invalid.

d10-value (i.e. the value for which 10% of the material has smaller grain size) seems most appropriate. We tried other equations as well, and found that the differences are not large compared to the differences to the IP-determined values (Zisser, 2005).

We show three curves determined from the IP data after the Börner model: two with the extreme values 2.8 and 4.6 for the exponent c, and one for $c=3.65$. This value gives the best least-squares fit in terms of log k values to the grain size determined data in the depth range between 3 and 11 m, thus neglecting data above the groundwater level. The other parameter, l, influences the result only marginally, and we used the standard value $l=0.1$ suggested for unconsolidated sediments. The mean groundwater electrical conductivity was determined to be approx. 0.1 S/m. The curve determined after the Slater and Lesmes model was calculated with the values for m and n which give the maximum hydraulic conductivites. The hydraulic conductivity determined from a pump test is also indicated. It was determined using the well indicated in Fig. 2, filtered within the aquifer (between 1 and 10 m depth), using a flow rate of 80 m^3/h. It may be considered an average value representative of the entire aquifer (Englert et al., 2000).

The specific inner surface S_{por} of the sediments is another parameter that can be determined from IP data. Since the hydraulic conductivity estimates strongly depend on S_{por}, it is an important intermediate parameter that is instructive to look at. Slater and Lesmes (2002a) obtained the following empirical equation, which implicitly enters into the hydraulic conductivity determination:

$$S_{por} = 2000(\sigma'')^p, \quad (6)$$

where $p=0.5\pm0.2$, S_{por} is given in μm^{-1} and σ'' in S/m. Börner et al. (1996) obtained the linear dependence given by Eq. (3). Fig. 10 shows the IP-determined S_{por} values, compared with S_{por} values determined from BET measurements (see Brunauer et al., 1938, for fundamentals on this method) on samples from borehole 32. In this case, Slater and Lesmes (2002a) allow a larger range for exponent p, resulting in a range for S_{por}, whereas Börner et al. (1996) did not provide an error estimate for the linear constant. The IP-determined S_{por} values match the BET-determined data quite well for both sets of equations.

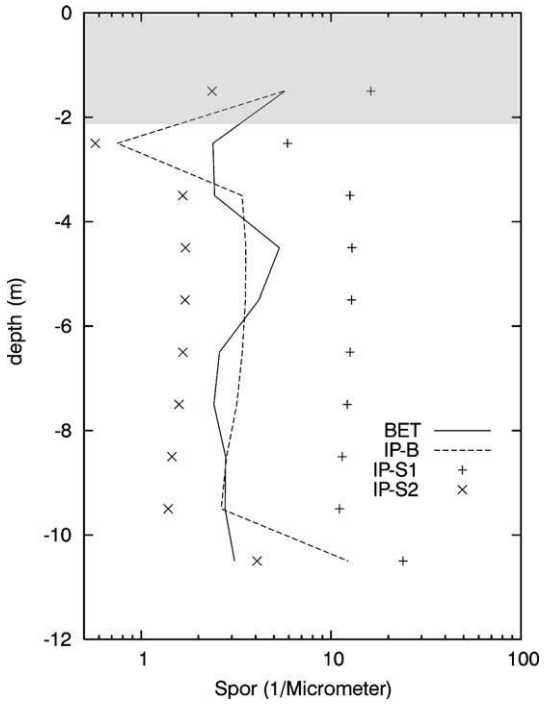


Fig. 10. Specific inner surface area at the location of borehole 32. Solid line: from BET measurements. Dashed line (IP-B): from Börner model. Symbols: from Slater and Lesmes model using exponents $p=0.5$ (IP-S1) and $p=0.7$ (IP-S2), respectively. The shaded area denotes the unsaturated zone where the equations are invalid.

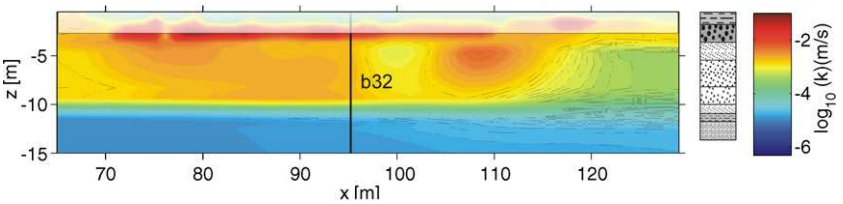


Fig. 11. Hydraulic conductivity section estimated from conductivity model shown in Fig. 7 using the Börner model with parameters $c=3.65$ and $l=0.1$. The blanking of the upper 2 m indicates the unsaturated zone, where the equations are supposed to be invalid. The average lithology has been inserted with proper scaling for comparison.

We calculated the hydraulic conductivities along the entire section from the Börner model (based on the 2-D complex conductivity inversion result shown in Fig. 7), using the optimum exponent c determined from the calibration with the grain size data. The result is shown in Fig. 11. Compared with the overall lithology, the image looks reasonable: increased hydraulic conductivities between 3 m and 11 m correspond with the known aquifer. The decreasing k values at 11 m are likely to be caused by the fine sands and the clay layer below. The clay layer at this depth is probably too thin to be resolved.

We used the same algorithm as described above to calculate hydraulic conductivities at the location of borehole b22 (Fig. 12). For exponent c of the Börner model, we used the value determined at borehole b32 ($c=3.65$). Calibration with one borehole and extrapolation into the area might be a suitable procedure if few boreholes are available. The IP-determined values with $c=3.65$ slightly (within an order of magnitude) overestimate k in the upper section of the aquifer (between 4 and 6 m) and slightly underestimate it in the lower section. The curve for the bestfitting exponent (based on log k data from 3 to 11 m, $c=3.0$) is also shown. The values obtained from the Slater and Lesmes model are substantially smaller than the estimates from grain size data. The inner surface areas for borehole b22 are

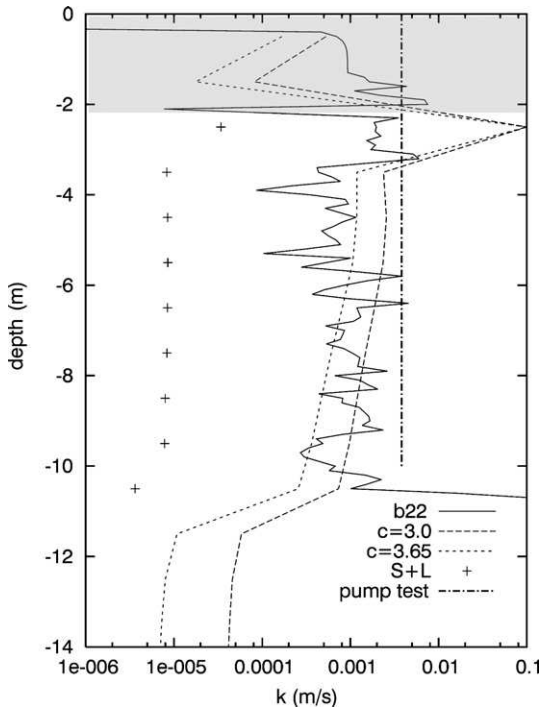


Fig. 12. Hydraulic conductivity at the location of borehole 22. Solid line: from grain size data using the Seiler-10 equation. Dashed lines: from the Börner model using different values of exponent c. Symbols: from the Slater and Lesmes model. Dash-dotted line: result from a pump test (Englert et al., 2000).

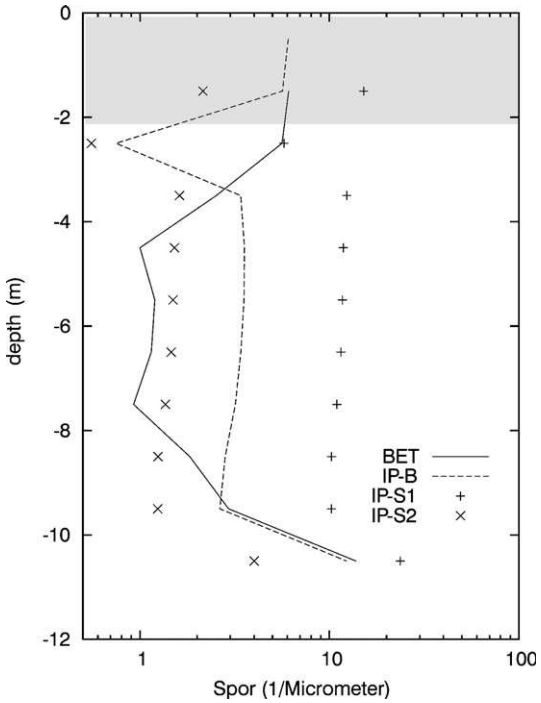


Fig. 13. Specific inner surface area at the location of borehole 22. Solid line: from BET measurements. Dashed line (IP-B): from Börner model. Symbols: from Slater and Lesmes model using exponents $p=0.5$ (IP-S1) and $p=0.7$ (IP-S2), respectively. The shaded area denotes the unsaturated zone where the equations are invalid.

compared with BET measurements in Fig. 13. At this location, the IP-determined values slightly overestimate the inner surface in the important depth range between 4 and 8 m, no matter which empirical equation is used.

5. Discussion

For both b32 and b22, the hydraulic conductivities determined from the Börner model fit the grain size determined values within an order of magnitude in the relevant depth range between 3 and 11 m. An order of magnitude estimate of hydraulic conductivites is generally considered difficult. Even if there is no possibility to calibrate exponent c, using an average value would not be too far off in the present case. When comparing hydraulic conductivities, we have to consider that values obtained from grain size data are only estimates based on empirical equations. Therefore, the results from the pump test indicated in Figs. 9 and 12 constitute an important additional verification. The average k of 3.8 10^{-3} m/s is slightly larger than the average that would be obtained from the IP-determined values. Considering that pump tests average over a large volume and zones with large hydraulic conductivity will dominate, the small discrepancy can be expected.

The values calculated after the Slater and Lesmes model are almost two orders of magnitude smaller, even though we used the parameters m and n which produce the maximum values within the range suggested by the authors. When comparing the two different sets of equations, we have to consider that Börner et al. (1996) were more conservative by allowing a larger range for their parameter c. However, even if we would allow a similar range for m and n, we would not get the Slater and Lesmes values to agree with the grain size determined data. Slater and Lesmes (2002a) already noted the discrepancy between their model and the Börner model. When they tried to fit the Börner model to their laboratory data, they obtained an exponent of $c=1.6$ for sands and sand/clay mixtures, and $c=0.9$ for tills, both of which are clearly out of the range between 2.8 and 4.6 suggested by Börner et al.

A full discussion of the difference, which is inherent in the laboratory results and not directly related to our data, is beyond the scope of this paper, but a closer look may provide some additional insight. The Slater and Lesmes samples consist of 4 sands, 5 tills, 5 alluvial silts/sands, and 17 artificial mixtures of till, sand and clay. Börner et al. (1996) do not describe their samples in detail, but the number of samples that enter into the parameter estimation is larger (>100), and their samples include a large variety of different sediment types (Weller, 2005, pers. comm). Therefore, the Slater and Lesmes data set might be more sensitive to a possible bias introduced by this particular set of samples. Another observation is that the Börner et al. data set includes more coarse-grained, high permeability samples. Their hydraulic conductivities span a range from approx. 10^{-6} to 10^{-3} m/s. The Slater and Lesmes data set ranges from 10^{-7} to 10^{-3} m/s, with only the 4 sand samples having values greater than 10^{-4} m/s. Within the Krauthausen aquifer, k ranges from 10^{-4} to 10^{-2} m/s, which is better covered by the Börner et al. data. This observation does not explain the inherent discrepancy between the two models, but it might motivate the investigation of sediments with large hydraulic conductivities in future laboratory studies.

Below 11 m, the estimate of the hydraulic conductivity strongly decreases, which is in agreement with the average lithology. Above 3 m, both IP-determined and grain size determined values increase, showing an apparent qualitative agreement. This might be coincidental. The sediments consist of a mixture of cobble and gravel, with some amounts of clay. Neither the grain size equations, nor the IP equations are supposed to be valid for this type of sediments, which show a large asymmetry in the gran size distribution. Above the water table, which is at 2.1 m, a comparison is not possible. The equations applied here are valid only for saturated conditions and can be expected to produce incorrect results. Since there is also an increasing interest in the unsaturated zone, these data might be relevant for future work.

Although for both b32 and b22 the IP-estimated hydraulic conductivities agree reasonably well with the grain size determined data, there are some differences in detail. At b32 (Fig. 9), the grain size data show a separation within the aquifer, with smaller values above 6 m, and larger values below. This is not resolved by the IP data, which exhibit little variation between 3 and 10 m. At b22 (Fig. 12), the grain size data do not show a clear separation within the aquifer, but slightly increasing values with depth, whereas the IP data decrease. The IP-estimated inner surface areas are very similar between b32 and b22 (Figs. 10 and 13), whereas the grain size determined values are consistently smaller in b22. Even though these differences are not huge, they indicate that there is a lateral variation in grain size distribution between b22 and b32 that is not resolved by our IP measurements. One possible explanation is that the 2-D inversion of parallel profiles might be insufficient to resolve those small variations, and a 3-D inversion might be required.

In Fig. 12, the determination of the best fit exponent ($c=3.0$) is slightly influenced by a zone around 10.5 m, where the grain size determined k values are unrealistically high. The outliers are caused by a small layer

with large uniformity coefficients (i.e. non-uniform grain size distribution), where the empirical equations to determine k from the grain size distribution are not valid. The outlier shows that it is not a trivial task to estimate hydraulic conductivity from grain size distributions, let alone a quantitative comparison with IP-determined values. Proper averaging of k with depth to determine a good representative exponent c is another difficult issue that might require extra efforts.

6. Conclusions

At the Krauthausen test site, the estimation of hydraulic conductivity using the empirical equations suggested by Börner et al. (1996) gives reasonable results that agree well with the known lithology. The equations include an adjustable parameter (c) which may vary between 2.8 and 4.6 and allows a wide range of possible values for k. In our particular case, the effect is not too dramatic, because our S_{por} values are relatively small (below 10 μm^{-1}). We would obtain acceptable order of magnitude estimates for k almost over the entire range of c. If more accurate information is required and borehole information is available, calibration of c (and l, which is less important) and extrapolating into the area, as we did here, might be one reasonable procedure.

We also tried an alternative equation to calculate k suggested by Slater and Lesmes (2002a). The k values determined this way are two orders of magnitude too small compared with results from grain size analyses and pump tests. Slater and Lesmes (2002a) discussed the difference of their equation with the Börner model and explained it by the different type of sediments used in the two studies. With our data, we are at the coarse-grained end of the equations, i.e. we have relatively large hydraulic conductivities and small imaginary electrical conductivities. For this end of the grain size spectrum our data seem to be in favour of the Börner model.

The equations used here are based on the assumption that the phase shift is constant over a wide frequency range. At the Krauthausen test site, this is partly fulfilled, but several data sets show a Cole–Cole type behaviour rather than following the constant-phase assumption. Even in the sample spectrum shown in Fig. 4, which we would categorise as a constant-phase type, a weak phase shift maximum is visible between 0.1 and 1 Hz. Suggestions have been made to estimate grain size distribution and hydraulic conductivity based on relaxation time (e.g. Kemna, 2000; Titov et al., 2002; Klitzsch, 2004; Kemna et al., 2005; Binley et al., 2005). Binley et al. (2005) observed a strong frequency dependence of the phase for sandstone samples from a UK triassic sandstone aquifer and concluded that the Börner model cannot be applied in their case. Clearly, the potential to extract additional information from the frequency dependence in an imaging framework should be exploited in future. This may be done either by parameterization of the intrinsic complex conductivities in terms of Cole–Cole parameters, or by inverting data from each frequency separately and calculation of relaxation times from the intrinsic spectra (Kemna et al., 1999). Both possibilities are discussed in Blaschek (2006).

An important advancement to obtain realistic models was a modification of the original inversion algorithm. By replacing the standard smoothness constraint with a focussing regularisation, sharp boundaries are no longer suppressed, and the images show distinct layers with smooth parameter variations within the layers. However, even with the modified constraint, the resolution of the method remains limited. Although our model nicely delineates the top and the bottom of the aquifer, we are unable to differentiate between the three different layers within the aquifer as described by Vereecken et al. (2000). Without constraints from borehole measurements, such a high resolution probably cannot be expected from surface electrical measurements.

Overall, we feel that our study encourages future work. Although we have data from only one type of lithology in one aquifer, field studies like this are important to assess possible limitations and practical difficulties. Another aspect is that the sediments under investigation remain undistorted, and thus our data are an important feedback for more systematic laboratory investigations in future. With the number of field studies increasing, it might even be possible to establish empirical equations derived from field data alone.

Acknowledgments

We thank Norbert Klitzsch, Andreas Englert and Tino Radic for their continuous support and many fruitful discussions. We are grateful to Harry Vereecken for the permission to work at the Krauthausen test site. The results were obtained within a joint project with Christoph Clauser, RWTH Aachen, who provided parts of the equipment. The GGA-institute, Hannover, provided equipment during an early stage of the project and Michael Grinat helped us to use it. We thank Andrew Binley and an anonymous reviewer for their constructive comments. The work was sponsored by the German Science Foundation (Projekt Ho1506/11-1).

References

Binley, A., Slater, L.D., Fukes, M., Cassiani, G., 2005. Relationship between spectral induced polarization and hydraulic properties of saturated and unsaturated sandstone. Water Resour. Res. 41, w12417, doi:10.1029/2005WR004202.

Blaschek, R., Hördt, A., Kemna, A., 2005. A new regularization for the inversion of IP data based on the minimum gradient support. 11th Eur. Mtg. Env. Eng. Geophys., Exp. Abstr.

Blaschek, R., 2006. Aspekte der Inversion von Daten der Spektralen Induzierten Polarisation. PhD. thesis, University of Bonn.

Börner, F.D., Schopper, J.R., Weller, A., 1996. Evaluation of transport and storage properties in the soil and groundwater zone from induced polarization measurements. Geophys. Prospect. 44, 583–601.

Brunauer, S., Emmett, P.H., Teller, E., 1938. Adsorption of gases in multimolecular layers. J. Am. Chem. Soc. 60, 309–319.

Dahlin, T., Leroux, V., Nissen, 2002. Measuring techniques in induced polarization imaging. J. Appl. Geophys. 50, 279–298.

Döring, U., 1997. Transport der reaktiven Stoffe Eosin, Uranin und Lithium in einem heterogenen Grundwasserleiter. Berichte des Forschungszentrums Jülich, vol. 3354. Forschungszentrum Jülich.

Englert, A., Hashagen, U., Jaekel, U., Nitzsche, O., Schwarze, H., Vereecken, H., 2000. Transport von gelösten Stoffen im Grundwasser-Untersuchungen am Testfeld Krauthausen. Grundwasser-Zeitschrift der Fachsektion Hydrogeologie, vol. 3, pp. 115–124.

Hallof, P.G., 1974. The IP phase measurement and inductive coupling. Geophysics 39, 650–665.

Hördt, A., Blaschek, R., Kemna, A., Suckut, J., Zisser, N., 2005. Hydraulic conductivity from spectral induced polarisation data — a case history. 18th Annual Meeting, SAGEEP. Exp. Abstr. , pp. 226–235.

Kemna, A., 2000. Tomographic inversion of complex resistivity — theory and application. PhD thesis, University of Bochum.

Kemna, A., Binley, A., 1996. Complex electrical resistivity tomography for contaminant plume delineation. 2nd Eur. Mtg. Env. Eng. Geophys., Exp. Abstr.

Kemna, A., Räkers, E., Dresen, L., 1999. Field applications of complex resistivity tomography. 69th Ann. Internat. Mtg., Soc. Expl. Geophys., Exp. Abst. 331–334.

Kemna, A., Binley, A., Slater, L., 2004. Crosshole IP imaging for engineering and environmental applications. Geophysics 69, 97–107.

Kemna, A., Münch, H.M., Titov, K., Zimmermann, E., Vereecken, H., 2005. Relation of SIP relaxation time of sands to salinity, grain size and hydraulic conductivity. 11th Eur. Mtg. Env. Eng. Geophys., Exp. Abst.

Klitzsch, N., 2004. Ableitung von Gesteinseigenschaften aus Messungen der spektralen induzierten Polarisation (SIP) an Sedimentgesteinen. PhD thesis, University of Leipzig.

Lesmes, D.P., Morgan, F.D., 2001. Dielectric spectroscopy of rocks. J. Geophys. Res. 106 (B7), 13329–13346.

Mazac, O., Cislerova, M., Vogel, T., 1985. A hydrogeophysical model for relations between electrical and hydraulic properties of aquifers. J. Hydrol. 79, 1–19.

Pelton, W.H., Ward, S.H., Hallof, P.G., Sill, W.R., Nelson, P.H., 1978. Mineral discrimination and inductive coupling removal with multifrequency IP. Geophysics 43, 588–609.

Portniaguine, O., Zhdanov, M.S., 1999. Focusing geophysical inversion images. Geophysics 64, 874–887.

Purvance, D., Andricevic, R., 2000. Geoelectrical characterisation of the hydraulic conductivity field and its spatial structure at variable scales. Water Resour. Res. 36 (10), 2915–2924.

Radic, T., 2004. Elimination of cable effects while multichannel SIP measurements. 10th Eur. Mtg. Env. Eng. Geophys., Exp. Abstr.

Radic, T., Kretzschmar, D., Niederleithinger, E., 1998. Improved characterisation of unconsolidated sediments under field conditions based on complex resistivity measurements. 4th Eur. Mtg.Env. Eng. Geophys., Barcelona, Exp. Abst.

Schön, J., 1996. Physical Properties of Rocks. Elsevier Science.

Seiler, K.-P., 1979. Durchlässigkeit und Porosität von Lockergesteinen in Oberbayern. Mitteilung zur Ing.-u. Hydogeologie 9, 105–126.

Slater, L.D., Glaser, D.R., 2003. Controls on induced polarization in sandy unconsolidated sediments and application to aquifer characterization. Geophysics 68, 1547–1588.

Slater, L.D., Lesmes, D.P., 2002a. Electric–hydraulic relationships observed for unconsolidated sediments. Water Resour. Res. 38 (10). doi:10.1029/2001WR001075.

Slater, L.D., Lesmes, D.P., 2002b. IP interpretation in environmental investigations. Geophysics 67, 77–88.

Titov, K., Komarov, V., Tarasov, V., Levitski, A., 2002. Theoretical and experimental study of time-domain induced polarisation in water-saturated sands. J. Appl. Geophys. 50, 417–433.

Vereecken, H., Döring, U., Hardelauf, H., Jaekel, U., Hashagen, U., Neuendorf, O., Schwarze, H., Seidemann, R., 2000. Analysis of solute transport in a heterogeneous aquifer: the Krauthausen field experiment. J. Contam. Hydrol. 45, 329–358.

Weller, A., Seichter, M., Kampke, A., 1996. Induced-polarization modelling using complex electrical conductivities. Geophysics 127, 387–398.

Xiang, J.N.B., Jones, D., Cheng, D., Schlindwein, F.S., 2002. A new method to discriminate between a valid IP response and EM coupling effects. Geophys. Prospect. 50, 566–576.

Yi, M.J., Kim, J.H., Chung, S.H., 2003. Enhancing the resolving power of least-squares inversion with active constraint balancing. Geophysics 68, 931–941.

Zisser, N., 2005. Bestimmung des kf-Wertes mit der spektralen induzierten Polarisation (SIP). Diplom thesis, University of Bonn.